MNRAS **000**, 1–8 (2019) Preprint 13 January 2020 Compiled using MNRAS LATEX style file v3.0

Detection of gamma-ray transients with wild binary segmentation

S. Antier[1,2], K. Barynova[2,3], P. Fryzlewicz[4], C. Lachaud[1], G. Marchal-Duval[2]
[1]*APC, Univ. Paris Diderot, CNRS/IN2P3, CEA/lrfu, Obs de Paris, Sorbonne Paris Cité, France*
[2]*LAL, Univ Paris-Sud, CNRS/IN2P3, Orsay, France*
[3]*Department of Physics, Taras Shevchenko National University, 03022 Kiev, Ukraine*
[4]*Department of Statistics, London School of Economics, Houghton Street, London WC2A 2AE, UK*

Last updated 2019 July 17; in original form 2019 July 18

ABSTRACT
In the context of time domain astronomy, we present an offline detection search of gamma-ray transients using a wild binary segmentation analysis called F-WBSB targeting both short and long gamma-ray bursts (GRBs) and covering the soft and hard gamma-ray bands. We use NASA Fermi/GBM archival data as a training and testing data set. This paper describes the analysis applied to the 12 NaI detectors of the Fermi/GBM instrument. This includes background removal, change-point detection that brackets the peaks of gamma-ray flares, the evaluation of significance for each individual GBM detector and the combination of the results among the detectors. We also explain the calibration of the ~ 10 parameters present in the method using one week of archival data. Finally, we present our detection performance result for 60 days of a blind search analysis with F-WBSB by comparing to both the on-board and offline GBM search as well as external events found by others surveys such as Swift-BAT. We detect 42/44 on-board GBM events but also other gamma-ray flares at a rate of 1 per hour in the 4-50 keV band. Our results show that F-WBSB is capable of recovering gamma-ray flares, including the detection of soft X-ray long transients. F-WBSB offers an independent identification of GRBs in combination with methods for determining spectral and temporal properties of the transient as well as localization. This is particularly useful for increasing the GRB rate and that will help the joint detection with gravitational-wave events.

Key words: Gamma-ray bursts, data analysis — wild binary segmentation

1 INTRODUCTION

The most recent LIGO/Virgo O2 observational campaign opened a new era of multi-messenger time-domain astronomy (The LIGO Scientific Collaboration et al. 2018, 2019) with the detection of a binary neutron star coalescence GW170817 on 2017 August 17 at 12:41:06 UT followed by a gamma-ray burst (GRB170817A) detected by the Fermi Gamma-ray Burst Monitor (GBM) (Abbott et al. 2017). GBM continuously observes the entire sky that is not occulted by the Earth in the band 4 keV - 40 MeV with a 2 microsecond timing resolution with its 12 NaI and 2 BGO detectors (Meegan et al. 2009). On-board, GBM continuous data searches have been developed to detect in real time GRBs at a rate of about 240 GRBs per year (Narayana Bhat et al. 2016). These GRBs detections have contributed to different joint analyses, including with other gamma-ray surveys like Swift-BAT (Kocevski et al. 2018) or Insight-HXMT (Zhao et al. 2018) but also to find gamma-ray counterpart of orphan afterglows detected by optical surveys (Lipunov et al. 2016) and for new optical facilities that will be operational in the next decade such as LSST and ZTF (Della Valle et al. 2018).

In the past with BATSE (Stern et al. 2002) and more recently with GBM, it has been demonstrated that the sample of gamma-ray bursts detected by the on-board triggering of the instrument is large, but it is still smaller than what it could be at its sensitivity (see GBM subthreshold analysis). Identifying the weaker GRBs may give a substantial increase of the GRB statistics : it may extend the log N-log Peak Flux to low Peak-flux and thus allow for the estimate of the total rate of GRBs in the universe. More importantly nowadays, with the emergence of the multi-messenger astronomy with the first joint GRB-GW detection, new analyses from the GBM team have been developed to detect gamma-ray counterparts of transient events. As an example, there is the LB15 method to search the detectors' continuous data for short transient events in temporal coincidence with LIGO/Virgo compact binary coalescence triggers (Blackburn et al. 2015; Burns et al. 2019). Others ground data analyses originate from Terrestrial Gamma-ray Flashes (TGFs) searches are looking for extra short GRBs in the GBM data (Briggs et al. 2015).

In this paper, we propose a new method, F-WBSB, for an independent blind ground analysis of the 12 NaI GBM detectors data. F-WBSB [1] is a search of weak and highly variable transient phenom-

[1] Fermi/GBM-like search with Wild Binary Segmentation for the detection of Bursts

ena in gamma-rays as GRBs. We interpret the statistical problem of detecting GRBs against an otherwise constant background as the problem of change-point detection, in the sense that the start- and end-points of the GRB are estimated separately as change-points against the constant background. This concept is not traditionally used by the standard methods of the GRB trigger literature (Blackburn et al. 2015; Burns et al. 2019; Savchenko et al. 2012). Non standard approachs (but not similar to our change-point method) have been investigated (Scargle 1998; Scargle et al. 2013). They use bayesian blocks algorithms for identifying structured variations similar to GRB profiles (Norris et al. 2005; Norris & Bonnell 2006; Hakkila & Preece 2011; Hakkila et al. 2014). Different approach can target different populations of GRBs. Indeed, the category of transient sources detected by an instrument depends not only on its design properties (detector surface, energy band, field of view), but also on the transient algorithm architecture. Besides, F-WBSB allows us to maintain a low computational complexity of the resulting method: change-point detection can typically be achieved in close to linear computational time in the number of data points, whereas a typical one-stage method for estimating both the start- and the end-point of a GRBs in a single pass through the data would need at least a quadratic computational complexity. Our approach is therefore computationally fast. It also preserves a linear high temporal resolution (e.g 128 ms) for the length of the sequence defined by start-end stops change-points which is not the actual case with classical methods using a $\{0.128, 0.256, 0.512, 1.024, ..s\}$ multi-scale resolution. Different methods of change-points have been proposed in the litterature (see as example Yao 1988; Killick et al. 2012). Here we perform our change-point analysis using the Wild Binary Segmentation (WBS) method of Fryzlewicz (2014), in light of its encouraging empirical performance. In addition, we use median smoothing for the evaluation of the gamma-ra background allowing flexibility to analyse longer transients in the count rate compared to previous methods in the astrophysical field as well as exploring the softer X-ray band below 50 keV. Finally, we conduct our analysis with a set of about 9 parameters, orthogonal to hundreds of parameters used in existing methods. In this paper, the F-WBSB procedure has been tested on 60 days of GBM daily records of available detector and energy bands. Then, we have compared our gamma-ray candidates with existing catalogs such as onboard Fermi-GBM, subthresholds, Swift-BAT, INTEGRAL-IBAS, Astrosat-CZTI, Konus-Wind and MAXI. This work is a first step toward detecting candidates of gamma-ray bursts or other astrophysical sources from background. First, the multiple independent detection among the 12 GBM detectors enables a low rate of cosmics. Secondly, the use of several energy bands gives a first idea of the nature of the transients (most of the X-ray galactic flares are detected below 50 keV). Finally the comparison with other catalog surveys demonstrates our capacity to find real events not detected by the Fermi GBM standard method. Our method aims to be integrated in systematic offline analyses for current missions such as GBM, SPI-ACS or HXMT but also for future mission such as SVOM (Wei et al. 2016). Jointly with a localization approach as shown in Berlato et al. (2019) or similar (Briggs et al. 2015), the method can be used for detecting new GRBs especially multi-peak and softer ones.

The paper is organized as follows. In Section 2, we describe the GBM data used to calibrate and test the method. In Section 3, we describe the F-WBSB general methodology and outline the WBS technique in more detail. In Section 4, we show the results of the calibration and parameters used for F-WBSB. In Section 5, we give our results concerning the detection of gamma-ray transients over 60 days of GBM data and compare with others surveys.

2 INPUT DATA

We evaluate F-WBSB detection performance using daily records from the twelve semi-directional sodium iodide (NaI) detectors of the GBM space instrument, covering an energy range of 4 - 5000 keV. We use the continuous Time-Tagged Event data (TTE), which gives a list of photons in each detector with time and energy channel information (128 energy resolution). We then build time series with a temporal resolution of 128 ms and 4 energy channels [4-50], [50-100], [50-900] and [4-900] keV.

GBM time series can be described as $\{X_t\}_{t\in[1,T]}$, with recorded events in one NaI detector, with N change-points where locations $\eta_1, ..., \eta_N$ correspond to high variations of the signal due to presence of variable or transient astrophysical sources. The canonical model of the signal is of the form :

$$\forall t \in [1,T],\ X_t = f_t + b_t \tag{1}$$

where f_t is a deterministic, one-dimensional, piecewise-constant signal with change-points, and the sequence b_t is the background noise with smoothly-variation expectation (not related to any variable or transient astrophysical event, see Section 3.2 for details).

3 F-WBSB PIPELINE

F-WBSB is a multi-resolution timing approach for searching for transient variation lasting from 128 ms to 50 s in the four energy bands mentioned above to target both short and long GRBs. We now list the stages of the method as shown in in Figure 1:

- **step 1 - science data**. We select portions of the GBM time series that are suitable to be analyzed: e.g outside the South Atlantic Anomaly for which detectors are turned off to preserve their lifetime (see Section 3.1).
- **step 2 - background estimation**. F-WBSB works on a flat time series trend. For this reason, we have to estimate $E(b_t)$ and subtract the background trend out before looking for any prompt excess as shown in Section 3.2. The background trend arises because of contaminants such as bright high-energy sources that come in and out of the wide field of view, in addition to location-dependent particle and Earth atmosphere effects.
- **step 3 - change-points**. We compute the number and locations of multiple change-points in the cleaned data (after background removal) as in Section 3.3. To this end, we use the WBS method of Fryzlewicz (2014). WBS does not require the choice of a window or span parameter and does not lead to a significant increase in computational complexity. The stopping criterion of WBS uses the *strengthened Schwarz Information Criterion*, which offers very good practical performance for rare phenomena.
- **step 4 - region of interest**. The list of change-points is processed into a list of region of timing interval interests (ROIs), whose start and stop are the pair of change-points that maximize the signal to noise ratio of the ROI.
- **step 5 - multiple detections**. Individual-detector ROIs are cross-matched in time. A multiple-detector trigger e.g gamma-ray trigger is created with ends as the intersection of individual detector triggers. An evaluation of its significance measuring the excess over the background is performed in the contributed detector time series.
- **step 6 - validation**. We proceed to an evaluation of the multiple-detector trigger reliability by comparing the different energy bands, the shape of the light curves, and a cross-match with onboard GBM and untargeted search results (Goldstein et al. 2016) as well as other survey transients such as BAT (Lien et al. 2016).

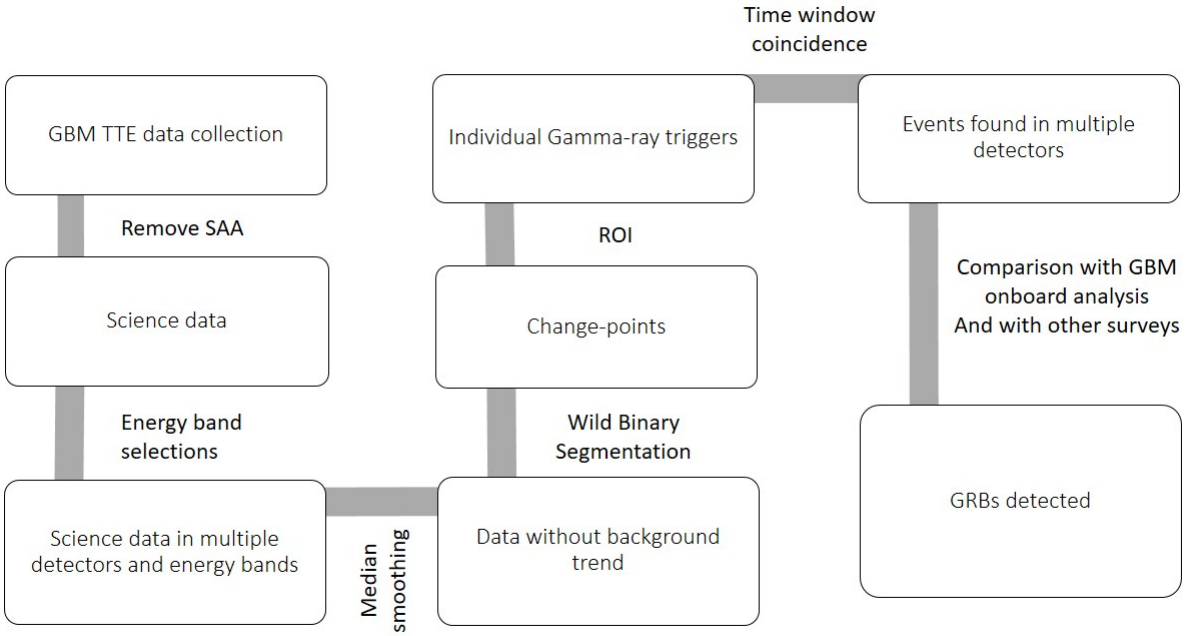

Figure 1. Flow chart of the F-WBSB procedure. First, we collect the raw data, and we remove portions of the daily sequence corresponding to the South Atlantic Anomaly. Then we compute various light curves in different energy bands from the raw data for the different NaI detectors. We estimate the background with median smoothing to have a flat variation of the time series. We investigate the change-point detection with the WBS approach (Fryzlewicz 2014). We construct different individual regions of interest (ROIs) and cross-match them in time to have obtain multiple-detector events.

After this overview of the pipeline, we describe the details of each step.

3.1 Science data

We select portions of the GBM time series outside the South Atlantic Anomaly (SAA) for which detectors are turned off and count rate is null (see Figure 2). We took a margin of 2.56 s at each end.

3.2 Background estimation

The GBM detectors are subject to a substantial time-varying background, due to:

- cosmic X-ray background as the highest contribution (Moretti 2009),
- bright high-energy sources that come in and out of the wide field of view,
- South Atlantic Anomaly trapped particles,
- other particle flux,
- Earth transit in the field of view and Earth atmospheric effects.

We note that the different contributions to the background depend on the spectral window; moreover, the background does not have a specific profile timing variation. In this analysis, the background is estimated for any time-interval (from milliseconds to dozen of minutes). We use a median smoothing filter that offers the possibility to follow the trend of GBM records. It is adaptable to any unexpected but relatively smooth variation of the background and differs from polynomial fitting approach in computing aspects and flexibility, and is not contaminated by high spikes of a GRB.

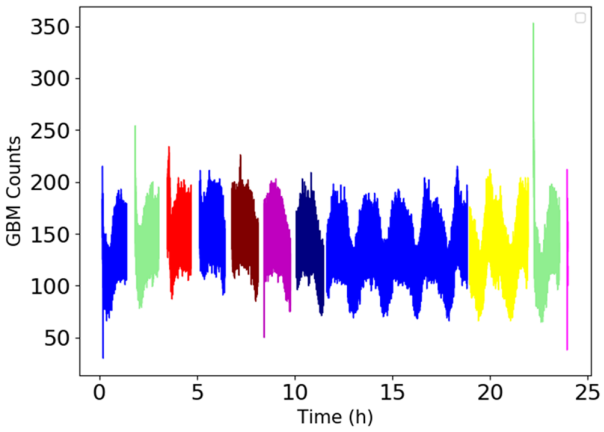

Figure 2. GBM counts detected (GBM NaI n_a detector) as a function of time (in hours) on September 4, 2018. Time bins are 0.128 s wide. The counts of the energy bands (from 4 keV to 5 MeV) are summed. The different colors represent the portions of the light curve that will be analyzed (outside the South Atlantic Anomaly).

The estimator $\tilde{E}(b_t)$ of $E(b_t)$ is of the form :

$$\tilde{E}(b_t) = \{\widehat{X_i}\}_{i\in[t-\frac{K-1}{2},t+\frac{K-1}{2}]}, \forall t \in [\frac{K-1}{2}+1, T-\frac{K-1}{2}] \quad (2)$$

with mirror-image padding at the left and right edge, where $\{\widehat{X_t}\}$ is the median of $\{X_t\}$ delimited by K, K is a parameter to be defined, depending on the timing resolution of $\{X_t\}$. For this analysis, K value is shown in Table 1.

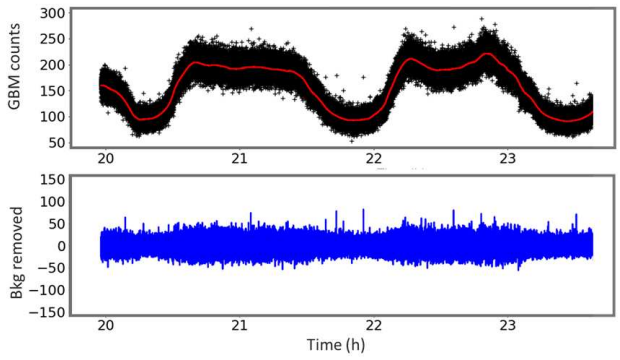

Figure 3. a) GBM counts detected (GBM NaI n_a detector) as a function of time (in hours) on September 1, 2018. Time bins are 0.128 s wide. The counts of the energy bands (from 4 keV to 5 MeV) are summed. The red line represents the median smoothing estimate ($K = 1025$, which corresponds to a median smoothing width of 130 s). b) Residual after background removal.

Figure 3 represents the underlying background continuum of a GBM detector, with 128 ms principally dominated by the cosmic X-ray background (in black), with an estimate of the background trend using median smoothing (in red), and corresponding residual data (in blue). Note that the value of the span K has been evaluated during the 7-day GBM training session (see Table 1 of Appendix A).

3.3 Change-point detection

F-WBSB searches for significant change-points in the count rate (X_t) recorded in GBM detectors for different energy bands. A pre-processing step has already removed the background trend (see Section 3.2). The remaining and unexpected variations of the cleaned signal could be caused by:

- a new transient source appearing in the field of view (the case we are interested in),
- high variability of X-ray sources present in the field of view,
- transit of X-ray sources on the edges of the field of view.

Change-points are determined by the WBS procedure as described in Fryzlewicz (2014). Two change-points could reveal the start or the stop of a new transient source, constituting an interesting case for the purpose of this study. Below we list the steps of the method as illustrated in Figure 4.

First, we define a set of M random time intervals whose start- and end- points have been drawn (independently with replacement) uniformly from the set $\{1, T\}$.

$$\begin{aligned} \forall m \in [1, M], \quad & [s_m, e_m] \subseteq [1, T] \\ \text{If } M = 1, \quad & [s, e] = [1, T] \end{aligned} \tag{3}$$

For each time interval $[s_m, e_m]_{m \in [1, M]}$, we compute the contrast weights vector. The inner product between this contrast vector and the vector $(X_{s_m}, ..., X_{e_m})$ is one of the basic ingredients of the wild binary segmentation algorithm. The *contrast* vector $\tilde{X}^u_{s_m, e_m}$ given at the time u is:

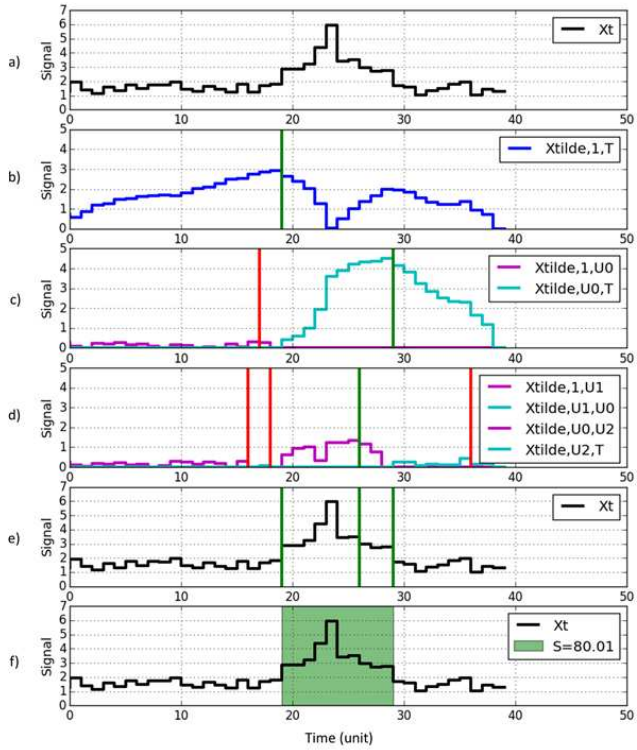

Figure 4. An example of the WBS iteration procedure. In steps a) to d), the change-point candidates are iteratively determined by computing $|\tilde{X}^u_{s_m, e_m}|_{u \in [s_m, e_m]}$, where $m \in [1, M]$. In this illustration, $M = 1$. They are then sorted from the most to the least important, and the N+1 most important ones, denoted by $\{\tilde{\tau}_i\}_{i \in [0, N]}$ and shown in green, are selected via the strengthened Schwarz Information Criterion. The rest, shown in red, are eliminated. Steps a) to d) use the WBS algorithm. Step d) shows the set of detected change-points. In step e), the most significant regions of interest (ROI) are represented, delimited by two change-points. The selection of contributed detectors will be done comparing the individual trigger times. Step f) shows the final ROI that is considered as a gamma-ray burst candidate.

$$\forall u \in [s_m, e_m], \; n = e_m - s_m + 1, \tag{4}$$

$$\tilde{X}^u_{s_m, e_m} = \sqrt{\frac{e_m - u}{n\,(u - s_m + 1)}} \sum_{t=s_m}^{u} X_t - \sqrt{\frac{u - s_m + 1}{n\,(e_m - u)}} \sum_{t=u+1}^{e_m} X_t \,.$$

We compute $(m_0, u_0) = \arg\max_{m,u \in \{s_m, ..., e_m - 1\}} |\tilde{X}^u_{s_m, e_m}|$. We add u_0 to the set of change-point candidates. The time domain [1,T] is then split into two sub-intervals to the left and to the right of u_0 (see step b in Figure 4). The recursion continues in this way (see step c and d in Figure 4) until all intervals $[s_m, e_m]$ have been examined (for the case $M > 1$) or until there are no more intervals to consider (for the case $M = 1$). We then order the change-points candidates from the most to the least important, according to the decreasing magnitude of $|\tilde{X}^{u_0}_{s_{m_0}, e_{m_0}}|$. We determine which of the most important change-points enter the set of change-points $\{\tilde{\tau}_i\}_{i=0}^{N}$ (see step e in Figure 4) through the so-called strengthened Schwarz Information Criterion, which is practically equivalent to the classical Schwarz (Bayesian) Information Criterion. If fewer than two change-points survive this selection, there are no burst candidates to speak of, and we stop. Otherwise, we next trigger the

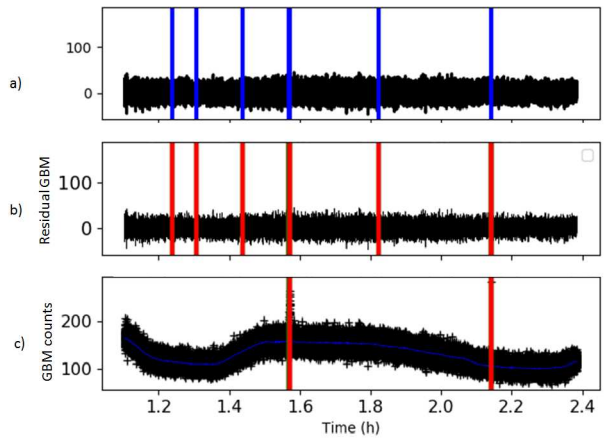

Figure 5. Residual (case a and b after background removal) GBM NaI n_2 detector counts as a function of time (in hours) on August, 08, 2017. Time bins are 0.128 s wide. The counts of the energy bands (from 4 keV to 900 keV) are summed. a) blue vertical lines represent the change-points with WBS b) green/red vertical lines represent list of ROI with start-and end-points (6 here) c) selection of the individual ROIs that pass the threshold $\mathrm{SNR}_{\mathrm{max}}$. Finally 2 ROIs selected.

procedure described in Section 3.4. Throughout the paper, we use $M = 5000$ shown in Table 1.

3.4 Creation of the region of timing interest and evaluation of its significance

We evaluate the significance of a region of timing interest (ROI) with the signal to noise ratio (SNR) delimited by two pairs of change-points (not necessarily adjacent) with:

$$\text{for i, j} \in [0, N], \ \mathrm{SNR}_{\tilde{\tau}_\mathrm{i}, \tilde{\tau}_\mathrm{j}} = \frac{\sum_{t=\tilde{\tau}_i}^{t=\tilde{\tau}_j} X_t - \tilde{E}(b_t)}{\sqrt{\sum_{t=\tilde{\tau}_i}^{t=\tilde{\tau}_j} \tilde{E}(b_t)}} \tag{5}$$

where $\{\tilde{\tau}_i\}_{i \in [0,N]}$ are change-point list found in previous step, X_t GBM single detector time series, $\tilde{E}(b_t)$ background trend estimation.

If $[\tilde{\tau}_i, \tilde{\tau}_j]_{i,j \in [0,N]} < \Delta_{\tilde{\tau}_i, \tilde{\tau}_j}$, and $\mathrm{SNR}_{\tilde{\tau}_i, \tilde{\tau}_j} > \mathrm{SNR}_{\mathrm{max}}$, then the ROI is selected as significant for the next step. For this analysis, $\mathrm{SNR}_{\mathrm{max}}$ and $\Delta_{\tilde{\tau}_i, \tilde{\tau}_j}$ values are shown in Table 1. Figure 5 represent the residual (cases a and b) and (step c) GBM daily data scan received in detectors (n_2) on September 8, 2008. The list of change-points detected are represented in case a) and the list of pairs of change points are listed in b). Finally, ROIs that passed the threshold $\mathrm{SNR}_{\mathrm{max}}$ are shown in c). Triggers around 1.56 hrs correspond to GRB170808065 as listed in Table A1 of Appendix A.

We flag as "1" timing portions for which a single ROI has been found in a certain energy band using the process above. At the end of the process, if the value is above 2, it means it is flagged as a multiple-detector event. We re-calculate the signal to noise ratio in the joint timing window for the contributed detectors. We then compare the multiple-detector event to different GRB databases such as GBM and BAT.

4 CALIBRATION OF F-WBSB

We run the F-WBSB method over 7 GBM daily data (from August 1 to August 7 2018 inclusive). Each data sequence is simultaneously analyzed for the NaI 12 count rates in the four energy bands mentioned. We calibrate F-WBSB with the help of the 11 gamma-ray events found by GBM onboard. Our results are shown in section in Table A1 of Appendix A. At the end of the calibration, all the parameters needed for this analysis are held constant (see Table 1). They are used for the 60-day F-WBSB performance described below.

Results of the blind search show that F-WBSB detect 11/11 GRBs from the onboard GBM analysis including long GRBs such as GRB180801492 and short GRBs such as GRB bn180801492. Note that F-WBSB found GRB180803590 in a single detection. We perform simulations for evaluating the false positive of the statistical background fluctuations. To do this, we create mock data using five full days (180808, 180809, 180907, 180810 and 180907). We compute a poissonian law distribution whose parameter was the median of any data science sequence in a given energy band. We run our F-WBSB analysis on the simulated data. We do not detect any multiple detection (two triggers found in the same time window of 60 s) for the different energy band. Our single detection rate (a detection in one detector) is at maximum 6 per day considering one energy band, leading a false positive rate of background fluctuations due to two detectors in coincidence at a level of 9 per year (with 60 s trigger time maximum separation).

5 BLIND SEARCH OF 60 GBM DAILY RECORDS

We run F-WBSB over 60 GBM days with held constant intrinsic parameters as discussed in Section 4: August 2017 (except 2017/08/20 and 2017/08/26, data not available), from 2018/08/08 to 2018/09/08. As shown in Table 2, F-WBSB detects more than 1000 events seen by at least two NaI detectors in 4-50 keV and 4-900 keV bands, and about 60 events in the 50-100 keV and 50-900 keV bands over this period. In parallel, we calculate the duty cycle of GBM (e.g period when scientific analysis is done with exclusion of the South Atlantic Anomaly) as 46.5 days. Trigger rates lead to about 30 events per day for the 4-50 keV band, 20 events per day for the 4-900 keV band, 1.2 event per day in the 50-100 keV and 50-900 keV bands. All the results are available at https://github.com/santier14/FWBSB/. Events have different astrophysical origins, such as galactic flares, cosmic rays (mainly in the 4-50 keV band), variable stars or gamma-ray bursts.

5.1 Comparison with GBM on-board analysis

F-WBSB detects 42 gamma-ray bursts out of 44 GRBs (3/4 of short GRBs) found by the GBM on-board analysis (see Table A2 of Appendix A). Most of the GRBs are seen in more than one energy band, but they represent 2/3 of the full F-WBSB events detected above 50 keV. Note that six GRBs are only recovered by a single detector event in the F-WBSB analysis. GRB170816258 and GRB170817529 are not detected by the blind F-WBSB search because no change-points were found at the GRB location. Nevertheless, we investigate locally without standard parameters, 10 minutes of data before the GRB170817529 trigger time until the next South Atlantic Anomaly passage happening a few minutes after GRB170817 reveals a multiple detection on n2 and n5 detectors with 1.152 s and 0.640 s durations respectively with a SNR of 6.1 in the 4 - 900 keV band.

Table 1. Parameters from the F-WBSB method set-up after 7-days GBM data investigation

Name	Unit	Value	Description
Energy bands	keV	4-50, 50-100, 50-900, 4-900	F-WBSB searches are run independently.
Minimal resolution	ms	128	Minimal resolution for F-WBSB search
Kernel Median (K)	s	130	Kernel used for Background fitting for 128 ms resolution
M		5000	random time intervals of WBS
N	/hours	3	Number of maximum change-points accepted
Δ_{τ_i,τ_j}	s	50	Maximum duration of F-WBSB duration
$\mathrm{SNR_{max}}$	-	3.0	SNR threshold of a single detector trigger

Table 2. F-WBSB results for the 60 days blind search analysis for August 2017 (except 2017/08/20 and 2017/08/26), from 2018/08/08 to 2018/09/08. The results are expressed in rates for all events found and for the joint F-WBSB and onboard GBM searches.

Energy bands	All triggers		GBM-WBS triggers	
	number	rate	number	rate
4-50 keV	1508	32.40 /d	32	0.67 /d
4-900 keV	1049	22.54 /d	39	0.84 /d
50-100 keV	58	1.25 /d	28	0.60 /d
50-900 keV	57	1.22 /d	35	0.75 /d

The number of detectors involved for the on-board GBM analysis can vary in the F-WBSB analysis due to variations in the background fit during online and offline searches. As an example, GRB170830069 is triggered by n_7 and n_b detectors with onboard GBM analysis whereas the GRB is clearly seen in n_6, n_9 and n_a as WBS reported in Table A2 of Appendix A.

The F-WBSB and GBM onboard analysis trigger times vary from less than 2 s for more than 50% of the 34 GRBs found in the 50-900 keV band. There is no clear preferential delay between the softer 4-50 keV band and the harder 50-900 keV band for the 32 GRBs found by F-WBSB. For example, GRB170804911 is found 12 s earlier by F-WBSB in the 4-50 keV band than GBM and F-WBSB hard trigger analysis (above 50 keV). In contrast, GRB180906597 is found 2 s delay in the 4-50 keV compared to F-WBSB 50-900 keV search.

Moreover, we also detect multi-episodes of 8 out of 9 long GRBs (T90 $>$ 100 s) which helps to recover its duration by identification. Indeed, F-WBSB configuration finds event/peak duration up to 50 s as mentioned in Table 1. Note GRB180826055 is detected by F-WBSB on detector n_9 at 01:17:22 e.g 123 seconds before the GBM trigger, with a detection of a precursor gamma-ray emission. We compare the duration of the F-WBSB event duration in the 4-900 and 50-900 energy band to the T_{90} GBM durations. More than 60% of GRBS recover more than 50% of the T_{90} in 50-300 keV for 34 GRBs found in 50-900 keV;20% have a trigger duration 10% longer than T_{90}. For 38 GRBs found in 4-900 keV, more than 80% of GRBS recover more than 50% of the T_{90} in 50-300 keV and 30% have a trigger duration 10% longer than T_{90}, showing the contribution to longer soft emission.

In conclusion, F-WBSB offers a unique and independent way to give a first classification of the gamma-ray triggers based on their trigger duration. Even if the method is focused on the discovery of new triggers, it provides a duration of the prompt emission of the gamma-ray transients in several bands. Moreover, it helps to understand the spectral dynamics of the prompt emission that is much more complex with a smooth transition from the hard to soft X-ray bands with the different delays and durations across the multi-band triggers (mostly below Δ_{τ_i,τ_j}=50 s). Further investigations are necessary to cleary identify the nature of the gamma-ray transients (e.g extra-galactic vs galactic sources) from the complete sample: we need an estimation of the location of the event, spectral properties and possible multi-wavelength counterpart.

5.2 Detection in coincidence with others surveys

F-WBSB also detects other events, especially in the softer band (4-50 keV). We perform some investigations by comparing F-WBSB events with other transients from gamma-ray surveys such as Fermi-GBM, subthresholds, Swift-BAT, Konus-Wind, HXMT, CALET and MAXI. We allow +/- 30 second latency in timing between the two gamma-ray events. Our F-WBSB detects jointly with GBM onboard analaysis 6 GRBs with Swift-BAT, 16+1 GRBs with Konus-Wind, 2 GRBs with MAXI, 2 GRBs with CALET and 6+1(galactic flare) GRBs with HXMT (see Table A1). Over the blind search period, F-WBSB does not detect gamma-ray events in coincidence with the 9 Swift-BAT GRBs, 22 X-ray MAXI flares, 6 HXMT GRBs, 7 Konus-Wind GRBs and no GRB170825 Agile GRB.

We also detect 6 events among the 54 events in timing coincidence with the sub-threshold analysis of Fermi-GBM listed in Table 3. Taking $\tau_{\mathrm{GBM}} = 54/46.5 = 1.16$/day and $\tau_{\mathrm{WBS}} = 32$/day and within a window of $\Delta_{\mathrm{coinc}} = 1\mathrm{min} = 6.9\times10^{-4}$ day, the accidental coincidence rate is $R_{\mathrm{fake,GBM}} = 0.03$ /day ($\approx$ 1.4 events for this analysis). Note that we consider F-WBSB and Fermi sub-threshold analysis as two independent studies, since the two approaches are very distinct, with an optimization on a short GRB investigation for the Fermi sub-threshold and a larger diversity GRB target for F-WBSB.

We detect four events correlated in time with Swift-BAT GRB but not found by onboard and offline GBM analysis.Table 3. Taking $\tau_{\mathrm{Swift}} = 90/365.25 = 0.25$/day and $\tau_{\mathrm{WBS}} = 32$/day and within a window of $\Delta_{\mathrm{coinc}} = 1\mathrm{min} = 6.9\times10^{-4}$ day, the accidental coincidence rate is $R_{\mathrm{fake,Swift}} = 0.006$ /day ($\approx$ 0.3 events for this analysis).

We also detect four events with F-WBSB in timing coincidence with events found by MAXI below 20 keV. Taking $\tau_{\mathrm{MAXI}} = 28/46.5 = 0.60$/day and $\tau_{\mathrm{FWBSB}} = 32$/day and within a window of $\Delta_{\mathrm{coinc}} = 1\mathrm{min} = 6.9\times10^{-4}$ day, the accidental coincidence rate is $R_{\mathrm{fake,MAXI}} = 0.01$ /day ($\approx$ 0.5 events for this analysis).

In conclusion, either for Swift-BAT and MAXI triggers, F-WBSB independent searches offer the possibility to extend the spectral range of the X-ray transients and variable stars observed thanks to the broad energy band coverage of GBM. For example, the joint analysis of GRB1808018A with BAT and GBM can help to estimate the E_{peak} parameter of the GRB spectrum. Also Swift localization is more accurate than GBM enabling spectroscopic follow-up and estimation of the redshift. In addition, comparison with multiple searches with independent false alarm rate estimation can confirm detections of weak signals. The joint F-WBSB and Fermi-GBM

Table 3. Results of the F-WBSB data analysis compared with Fermi-GBM subthresholds. From the 54 sub-thresholds triggers, 6 were also found by F-WBSB listed above.

GBM Name and ref	Day	GBM Trigger Time (UT)	F-WBSB Trigger Time (UT)	F-WBSB Duration (s)	F-WBSB Detector involved	F-WBSB SNR	F-WBSB Energy band (keV)	F-WBSB ref
556027113	2018/08/15	11:58:28.82	11:59:10.66	8.064	n2,na	53.7	4-50, 4-900, 50-100	Link
525514019	2017/08/27	08:06:54.63	08:06:01.28	0.512	n5	9.8	4-50	Link
525127039	2017/08/22	20:37:14.70	20:37:39.38	0.512	n0	3.5	4-900	Link
524798902	2017/08/19	01:28:17.06	01:28:16.19	1.664	n3	6.0	4-900	Link
524556701	2017/08/16	06:11:36.23	06:11:54.18	2.048	n7	6.9	4-900	Link
523661895	2017/08/05	21:38:09.49	21:38:09.49	1.408	n6	6.6	50-100, 50-900	Link

Table 4. Results of the F-WBSB data analysis compared with Swift-BAT when Fermi-GBM onboard did not trigger. From the 18+1(classified as galactic) Swift-BAT GRBs triggers, 6 have been detected jointly by Fermi-GBM and F-WBSB (see Table A1), and 4 with F-WBSB only reported here.

BAT Name and ref	Day	BAT Trigger Time (UT)	F-WBSB Trigger Time (UT)	F-WBSB Duration (s)	F-WBSB Detector involved	F-WBSB SNR	F-WBSB Energy band (keV)	F-WBSB ref
GRB170807A	2017/08/07	21:56:09.11	21:55:48.93	0.64	n4,n5	31.2	4-50	Link
GRB180805A	2018/08/05	09:04:49.02	09:04:48.83	1.92	n2	6.2	4-50	Link
GRB180818A	2018/08/18	03:12:04.03	03:12:03.01	6.66	n0	6.1	4-50	Link
GRB180905A	2018/09/05	13:57:46.45	13:58:54.0	7.68	n3,n8	7.0	4-900	Link

subthreshold analysis are helpful for multi-messenger studies as for GW150914-GBM discussion (Connaughton et al. 2016).

5.3 Additional detection from F-WBSB

F-WBSB also detects multiple events mainly in the soft band at a rate of 32 events per day in the 4-50 keV band. They are mainly due to variable stars and X-ray galactic flares. We investigate every event to check if it is not due to the approximate background estimation. However, without localization, it is hard to find the nature of the transient events. Nevertheless, we collect 171 events found by F-WBSB checking by hand the profile of those events. They are not found by other gamma-ray surveys compatible with GRB lightcurves provided in here. Among the 171 events, 95% of the events are 4-50 keV events, 70% of the events are in the 4-900 keV band and 0.5% of the events are in the 50-900 and 50-100 keV bands. This sample has a low enough rate to be helpful in the future for cross-matching a sample of transients in other wavelengths such as orphan visible afterglows or other messengers such as gravitational waves and neutrinos.

6 DISCUSSION AND CONCLUSION

In this paper, we present F-WBSB, an automatic blind search for detecting of gamma-ray transients. It is particularly sensitive to spiky gamma-ray transients in the soft X-ray band. F-WBSB uses a unique technique of gamma-ray detection with wild binary segmentation of a timing series and less than intrinsic 10 parameters to tune. We evaluated its performance using 60 days of Fermi-GBM continuous daily data, for the 12 NaI detectors records after one week of calibration. In addition, multi-band searches encourage a low signal-to-noise identification of the spectral characteristics with hard peaks in the 50-900 keV band and shorter duration events, and longer duration events for soft band or detection of additional triggers generally delayed from the harder band. Independent continuous searches are a powerful tool to discard weak fluctuations of the background and weak gamma-ray transients. By increasing GBM's sensitivity, the detected GRB rate can be increased (as the count of localisation). In addition, this approach is helpful to validate low signal-to-noise GRB signals in GBM data in coincidence with gravitational-wave detections, which is important for multi-messenger studies of the violent Universe. The results performance of the F-WBSB analysis reveals the detection of 42 events in the 4-900, 50-100, 4-50 or 50-100 keV bands in coincidence in time with the on-board GBM analysis out of 44 gamma-ray transients found by GBM onboard. Short GRBs are less clearly identified as compared to long GRBs due to the minimal resolution of 128 ms of F-WBSB compared to the 64 ms in on-board analysis. However, the multiple band peak detection in F-WBSB recovers more than 70% of the duration of 7 out of 9 GRBs with T90 $>$ 100s (50-300 keV) present in the sample. F-WBSB detects other gamma-ray transients at a rate of 30 events per day for the 4-50 keV band, 20 events per day for the 4-900 keV band, 1.2 event per day in the 50-100 keV and 50-900 keV bands. F-WBSB is able to recover GRBs found by the online on-board analysis and other surveys. But F-WBSB also finds events in time coincidence with other gamma-ray surveys while none are detected from online and offline GBM searches: one confident event seen by Swift-BAT (GRB180818A) and 4 others sub-threshold events found in coincident with Swift GRBs; there are also 4 F-WBSB events connected to MAXI galactic flares. A list of 171 events found by F-WBSB is unique and compatible with galactic or GRB light curve profiles. However, further investigations are required to determine the nature of the gamma-ray transient. For this purpose, new gamma-ray transient needs to be compatible with a extra-galactic source using rough localization (Berlato et al. 2019), GRB spectrum (e.g Band model) and timing profile. This also helps for the deeper classification of the transient as short and long GRBs or intermediate GRB classes (Mukherjee et al. 1998), that might differ in terms of progenitors (coalescence of neutrons stars vs coalescence of massive stars).

Recently, a systematic analysis of F-WBSB over 24h is performed in case of a gravitational wave alert during the third observational campaign of LIGO-Virgo since April 2019. No gamma-ray trigger is found in the period of around the GW trigger time (-5s, 1h) for the first six months (Antier et al. 2019). Indeed, this strategy gives a playground for multi-messenger searches with neutrino and gravitational-wave events as well as more broadly in time domain astronomy that will certainly help for identifying the nature of mil-

Table 5. Results of the F-WBSB data analysis compared with MAXI when Fermi-GBM onboard did not trigger. During the data analysis period, 28 events were detected by MAXI. 4 triggers were related to GRBs whereas the others are connected to flare stars. GRB170830A and GRB180809A were detected jointly by GBM-onboard and F-WBSB (see Table A1)

MAXI Name and ref	Day	MAXI Trig. Time (UT)	F-WBSB Trig. Time (UT)	F-WBSB Durat. (s)	F-WBSB Detec. involved	F-WBSB SNR	F-WBSB Energy band (keV)	F-WBSB ref
J1621-501	2018/09/02	05:02:29	05:01:38.5	42.624	n3,n6	6.8	4-900	Link
J1621-501	2018/08/05	11:37:03	11:37:19.42	0.512	n5	33.3	4-50	Link
4U 1916-053	2018/08/02	09:36:57	09:36:54.08	6.272	na	7.6	4-900	Link
H 1743-322	2017/08/06	09:54:14	09:54:27.26	23.296	n5	9.7	4-900	Link

lion of optical transients, including those from LSST (Della Valle et al. 2018).

ACKNOWLEDGEMENTS

SA is supported by the CNES Postdoctoral Fellowship at Laboratoire AstroParticule et Cosmologie. SA and CL acknowledge the financial support of the UnivEarthS Labex program at Sorbonne Paris Cité (ANR-10-LABX-0023 and ANR-11-IDEX-0005-02). We acknowledge the Laboratoire de l'Accélérateur Linéaire that provides founding KB for her internship. The work of PF was supported by the Engineering and Physical Sciences Research Council grant no. EP/L014246/1.

This paper has been typeset from a TEX/LATEX file prepared by the author.

REFERENCES

Abbott B. P., et al., 2017, ApJ, 848, L13
Antier S., et al., 2019, arXiv e-prints, p. arXiv:1910.11261
Berlato F., Greiner J., Burgess J. M., 2019, ApJ, 873, 60
Blackburn L., Briggs M. S., Camp J., Christensen N., Connaughton V., Jenke P., Remillard R. A., Veitch J., 2015, The Astrophysical Journal Supplement Series, 217, 8
Briggs M., et al., 2015, in EGU General Assembly Conference Abstracts. p. 9961
Burns E., et al., 2019, ApJ, 871, 90
Connaughton V., et al., 2016, ApJ, 826, L6
Della Valle M., et al., 2018, MNRAS, 481, 4355
Fryzlewicz P., 2014, Ann. Statist., 42, 2243
Goldstein A., Burns E., Hamburg R., Connaughton V., Veres P., Briggs M. S., Hui C. M., The GBM-LIGO Collaboration 2016, arXiv e-prints,
Hakkila J., Preece R. D., 2011, ApJ, 740, 104
Hakkila J. E., Preece R. D., Loredo T. J., Wolpert R. L., Broadbent M. E., 2014, in American Astronomical Society Meeting Abstracts #223. p. 352.11
Killick R., Fearnhead P., Eckley I. A., 2012, Journal of the American Statistical Association, 107, 1590
Kocevski D., et al., 2018, ApJ, 862, 152
Lien A., et al., 2016, ApJ, 829, 7
Lipunov V. M., et al., 2016, MNRAS, 455, 712
Meegan C., et al., 2009, ApJ, 702, 791
Moretti A., 2009, in Rodriguez J., Ferrando P., eds, American Institute of Physics Conference Series Vol. 1126, American Institute of Physics Conference Series. pp 223–226 (arXiv:0811.1444), doi:10.1063/1.3149419
Mukherjee S., Feigelson E. D., Jogesh Babu G., Murtagh F., Fraley C., Raftery A., 1998, ApJ, 508, 314
Narayana Bhat P., et al., 2016, ApJS, 223, 28
Norris J. P., Bonnell J. T., 2006, ApJ, 643, 266
Norris J. P., Bonnell J. T., Kazanas D., Scargle J. D., Hakkila J., Giblin T. W., 2005, ApJ, 627, 324
Savchenko V., Neronov A., Courvoisier T. J. L., 2012, A&A, 541, A122
Scargle J. D., 1998, ApJ, 504, 405
Scargle J. D., Norris J. P., Jackson B., Chiang J., 2013, ApJ, 764, 167
Stern B. E., Tikhomirova Y., Kompaneets D., Svensson R., 2002, in Gurzadyan V. G., Jantzen R. T., Ruffini R., eds, The Ninth Marcel Grossmann Meeting. pp 2440–2441, doi:10.1142/9789812777386_0605
The LIGO Scientific Collaboration et al., 2018, arXiv e-prints, p. arXiv:1811.12907
The LIGO Scientific Collaboration et al., 2019, arXiv e-prints, p. arXiv:1901.03310
Wei J., et al., 2016, arXiv e-prints, p. arXiv:1610.06892
Yao Y.-C., 1988, Statistics & Probability Letters, 6, 181
Zhao Y., et al., 2018, Research in Astronomy and Astrophysics, 18, 057

APPENDIX A:

Table A1. Calibration sample: results of the F-WBSB data analysis (August 2018) compared with the onboard GBM analysis (Narayana Bhat et al. 2016). The GRBs mentioned above were used as reference to calibrate F-WBSB parameters.

Search	Detectors Involved	Time (UT)	Trigger Duration (s)	SNR	Energy band (keV)	GRB classification	Ref
			bn180801276				
GBM onboard	n6,n7,n8,n9	06:37:04.51	0.064	5.7	47-291	long	Notice
F-WBSB	n6,n8	06:37:03.30	0.768	9.1	50-900		Link
			bn180801492				
GBM onboard	n0,n1	11:48:42.17	1.024	4.8	47-291		Notice
F-WBSB	n0,n3	11:48:41.30	8.064	17.2	4-50		
F-WBSB	n0, n3	11:48:43.80	5.12	9.8	50-100	long	Link
F-WBSB	n1	11:48:41.70	8.064	8.1	50-900		
F-WBSB	n0,n1,n3,n9	11:48:41.00	7.936	17.6	4-900		
			bn180803590				
GBM onboard	n3,n4	14:09:49.73	0.256	4.8	47-291		Notice
F-WBSB	n3	14:10:01.66	0.768	71.8	4-50	short	Link
F-WBSB	n3	14:10:01.66	0.768	56.5	4-900		
			bn180804554				
GBM onboard	n4,n5	13:17:41.44	2.048	4.9	47-291		Notice
F-WBSB	n4,n5	13:17:48.99	17.664	16.5	4-50		
F-WBSB	n1,n4,n5	13:17:45.80	5.12	17.4	50-100	long	Link
F-WBSB	n4,n5	13:17:38.24	29.696	32.2	50-900		
F-WBSB	n0,n4,n5	13:17:37.60	7.936	24.0	4-900		
			bn180804765				
GBM onboard	n2,n5	18:22:19.65	4.096	5.2	47-291		Notice
F-WBSB	n2,n5	18:22:13.18	17.92	9.0	4-50	long	Link
F-WBSB	n2,n5	18:22:14.34	15.744	10.6	4-900		
			bn180804909				
GBM onboard	n2,n5	21:49:02.18	4.096	4.7	47-291		Notice
F-WBSB	n1	21:48:04.67	36.224	8.2	50-900	long	Link
F-WBSB	n1,n2,n5	21:48:57.79	7.68	6.1	4-900		
			bn180804931				
GBM onboard	n8,nb	22:20:38.28	0.256	4.9	47-291		Notice
F-WBSB	n8,nb	22:20:37.10	13.056	10.2	4-50		
F-WBSB	n7,n8,nb	22:20:37.41	15.9	12.0	50-100	long	Link
F-WBSB	n3,n4,n6	22:20:36.44	21.632	7.9	50-900		
F-WBSB	n3,n4,n5,n8,nb	22:20:36.85	19.7	13.0	4-900		
			bn180805543				
GBM onboard	n6,n7	13:02:36.52	0.064	5.0	47-291		Notice
F-WBSB	n7	13:02:36.61	0.512	5.6	50-100		
F-WBSB	n6,n8,na	13:02:36.61	0.512	4.9	50-900	short	Link
F-WBSB	n7	13:02:36.35	0.896	9.9	4-900		
Swift-BAT	-	13:02:36.48	0.256	28.0	50-350		Notice
			bn180806665				
GBM onboard	n6,n8	15:57:58.30	2.048	5.0	47-291	long	Notice
F-WBSB			No detection				
			bn180806944				
GBM onboard	n7,n8	22:38:59.66	4.096	5.2	47-291		Notice
F-WBSB	n6,n7,n8,nb	22:38:46.08	29.184	63-62	4-50		
F-WBSB	n6,n7,n8	22:38:57.35	18.304	41.8	50-100	long	Link
F-WBSB	n7,n8	22:38:57.47	24.32	62.9	50-900		
F-WBSB	n7,n8,n9,nb	22:38:56.58	19.456	59.7	4-900		
			bn180807097				
GBM onboard	n8,na	02:19:54.72	2.048	5.1	47-291		Notice
F-WBSB	na,nb	02:19:41.51	38.656	8.9	4-50		
F-WBSB	na	02:19:52.77	4.992	5.8	50-100	long	Link
F-WBSB	n8,na,nb	02:19:51.36	4.096	6.3	50-900		
F-WBSB	n8,na,nb	02:19:50.21	9.216	10.3	4-900		

Table A2. Results of the F-WBSB data analysis (August 2017, August 2018 and September 2018) compared with the onboard GBM analysis. As an indication, other surveys that independently triggered on the same gamma-ray bursts as HXMT, Swift-BAT, Konus-Wind, Calet and MAXI are reported as well.

Search	Detectors Involved	Trigger Time (UT)	Trigger Duration (s)	SNR (av)	Energy band (keV)	GRB classification	Ref
		August 2017					
		bn170801690					
GBM onboard	n8,nb	16:33:43.40	2.048	4.5	47-291	long	Notice
F-WBSB	n7,n8,nb	16:33:40.80	4.224	7.4	4-900		Link
		bn170802638					
GBM onboard	n6,n8	15:18:24.80	0.064	5.0	47-291		Notice
F-WBSB	n7	15:18:26.24	0.512	11.0	4-50		
F-WBSB	n3,n4,n6,n7,n8,n9,na,nb	15:18:26.37	1.152	16.4	4-900		Link
F-WBSB	n3,n7	15:18:26.38	0.896	14.0	50-100	short	
F-WBSB	n3,n4,n6,n8,n9,na,nb	15:18:26.24	1.152	19.1	50-900		
HXMT	-	15:18:26.00	0.977	-	80-800		-
Konus-WIND	-	15:18:28.10	0.38	-	50-200		-
		bn170803172					
GBM onboard	n0,n1	04:07:15.75	2.048	5.4	47-291	long	Notice
F-WBSB	n1	04:07:14.63	1.408	6.9	50-100		Link
		bn170803415					
GBM onboard	n8,nb	09:57:44.26	1.024	5.0	47-291		Notice
F-WBSB	n7,n8,nb	09:57:40.80	77.056	12.7	4-50		
F-WBSB	n7,n8,nb	09:57:41.82	62.848	15.0	4-900	long	Link
F-WBSB	n6,n8,nb	09:57:42.60	50.297	10.0	50-100		
F-WBSB	n6,n7,n8,nb	09:57:40.81	72.704	7.3	50-900		
		bn170803729					
GBM onboard	n1,n3	17:30:27.11	0.064	5.6	47-291		Notice
F-WBSB	n0,n1,n3,n4,n5	17:30:26.75	4.480	14.6	4-50		
F-WBSB	n0,n1,n3,n4,n5,n6	17:30:26.62	4.992	19.5	4-900	long	Link
F-WBSB	n0,n1,n2,n3,n4,n5,n6	17:30:26.63	2.944	14.9	50-100		
F-WBSB	n0,n1,n3,n5,n6	17:30:26.63	4.736	42.5	50-900		
Swif-BAT	-	17:30:27.17	0.064	32.6	25-100		Notice
Konus-WIND	-	17:30:22.76	2.054	-	50-200		-
		bn170804911					
GBM onboard	n4,n8	21:52:21.46	2.048	4.7	47-291		Notice
F-WBSB	n4,n8	21:52:09.15	26.368	14.5	4-50		
F-WBSB	n4,n8	21:52:17.98	14.720	18.8	4-900	long	Link
F-WBSB	n4,n8	21:52:20.16	11.520	10.9	50-100		
F-WBSB	n4,n8	21:52:20.80	10.368	11.3	50-900		
		bn170805901					
GBM onboard	n6,n9	21:37:49.59	1.024	4.5	47-291		Notice
F-WBSB	n6,n7,n9	21:37:48.22	3.072	7.4	4-900	long	Link
F-WBSB	n6,n9	21:37:48.86	21.76	3.8	50-900		
		bn170808065					
GBM onboard	n2,na	01:34:09.39	0.512	4.6	47-291		Notice
F-WBSB	n2,na	01:34:09.85	7.552	11.3	4-50		
F-WBSB	n1,n2,n8,n9,na	01:34:07.67	5.760	13.3	4-900	long	Link
F-WBSB	n1,na	01:34:08.37	5.120	12.1	50-100		
F-WBSB	n1,n2,n7,n8,n9,na	01:34:07.22	6.016	11.1	50-900		
Konus-WIND	-	01:34:13.07	5.25	-	50-200		-
		bn170808936					
GBM onboard	n1,n5	22:27:43.10	0.512	5.2	47-291		Notice
F-WBSB	n9,na	22:27:01.18	43.392	6.3	4-50		
F-WBSB	n9,na	22:27:02.85	40.704	3.9	4-900	long	Link
F-WBSB	n0,n1,n2,n3,n5	22:28:06.73	3.58	10.2	50-100		
F-WBSB	n1,n5	22:28:05.83	45.568	1.0	50-900		
Konus-WIND	-	22:27:39.19	17.718	-	50-200		Notice

Table A2 – *continued* Results of the F-WBSB data analysis (August 2017, August 2018 and September 2018) compared with the onboard GBM analysis. As an indication, other surveys that independently triggered on the same gamma-ray bursts as HXMT, Swift-BAT, Konus-Wind, Calet and MAXI are reported as well.

Search	Detectors Involved	Time (UT)	Trigger Duration (s)	SNR (av)	Energy band (keV)	GRB classification	Ref
			August 2017				
			bn170810918				
GBM onboard	n0,n1	22:01:41.58	0.256	4.5	47-291	long	Notice
F-WBSB	n0,n1	22:01:16.10	70.4	9.2	4-900		
F-WBSB	n0,n1,n2	22:01:34.41	47.232	7.9	50-100		Link
F-WBSB	n0,n1,n2	22:01:31.20	54.016	11.9	50-900		
Swif-BAT	-	22:01:41.06	1.024	23.32	25-100		Notice
			bn170813051				
GBM onboard	n0,n1,n2,n3	01:13:08.80	0.512	4.6	47-291	long	Notice
F-WBSB	n1,n2	01:13:06.11	23.168	6.4	4-50		
F-WBSB	n0,n1,n2,n4	01:13:06.62	25.856	11.7	4-900		Link
F-WBSB	n0,n1	01:13:06.63	30.208	14.9	50-900		
Swif-BAT	-	01:13:16.48	64	12.3	15-50		Notice
			bn170816258				
GBM onboard	n5,n8	06:11:11.88	2.048	4.7	47-291	long	Notice
F-WBSB			No detection				
			bn170816599				
GBM onboard	n7,n8,na,nb	14:23:03.96	0.016	10.6	47-291	short	Notice
F-WBSB	n6,n7,n8,na,nb	14:23:03.74	2.176	13.9	4-900		Link
F-WBSB	n3,n6,n7,n8,n9,na,nb	14:23:03.62	0.896	17.1	50-900		
CALET	-	14:23:03.81	0.5	9.8	40-230		Notice
Konus-Wind	-	14:23:09.11	1.486	-	50-200		Notice
			bn170817529				
GBM onboard	n1,n2,n5	12:41:06.47	0.256	4.8	47-291	short	Notice
F-WBSB			No detection				
			bn170817908				
GBM onboard	n2,n5	21:47:34.43	0.032	7.9	47-291	long	Notice
F-WBSB	n0,n1,n2,n5	21:47:33.31	3.456	11.4	4-50		
F-WBSB	n0,n1,n2,n5,n9	21:47:33.31	0.256	11.5	4-900		Link
F-WBSB	n0,n1,n2,n4,n5,n8,n9	21:47:32.98	3.584	11.4	50-100		
F-WBSB	n0,n1,n2,n5	21:47:33.22	0.256	10.6	50-900		
HXMT	-	21:47:34.00	2.67	-	80-800		Notice
Konus-WIND	-	21:47:34.02	2.694	-	50-200		-
			bn170818137				
GBM onboard	n8,nb	03:17:19.98	0.064	5.8	47-291	short	Notice
F-WBSB	n8	03:17:19.68	0.896	6.0	50-100		Link
			bn170821265				
GBM onboard	n1,n9	06:22:00.85	2.048	4.9	47-291	long	Notice
F-WBSB	n0,n1,n9,na	06:22:02.18	21.632	8.1	4-50		
F-WBSB	n1,n9	06:21:58.47	25.344	10.9	4-900		Link
F-WBSB	n1,n9	06:21:58.34	10.368	8.5	50-100		
F-WBSB	n9	06:21:57.70	11.008	8.0	50-900		
			bn170825307				
GBM onboard	n3,n7	07:22:01.42	1.024	4.6	47-291	long	Notice
F-WBSB	n3,n6,n8	07:22:00.26	8.448	8.7	4-50		
F-WBSB	n3,n4,n6,n7,n8	07:22:00.77	5.76	16.7	4-900		Link
F-WBSB	n3,n4,n6,n7	07:22:00.52	6.016	9.8	50-100		
F-WBSB	n3,n4,n5,n6,n7,n8,na	07:21:59.62	6.784	13.5	50-900		
HXMT	-	07:22:03.00	4.77	-	80-800		-
Konus-WIND	-	07:22:06.22	6.345	-	50-200		-
			bn170825500				
GBM onboard	n6,n8	12:00:06.00	0.512	5.9	47-291	long	Notice
F-WBSB	n4,n5,n6,n7,n8,nb	12:00:05.18	9.344	44.0	4-50		
F-WBSB	n3,n4,n5,n6,n9,nb	12:00:05.31	3.712	13.9	4-900		Link
F-WBSB	n6,n7,nb	11:59:31.26	42.624	6.8	50-100		
F-WBSB	n3,n6,n7,n8,n9,nb	12:00:01.60	7.552	9.4	50-900		
Konus-WIND	-	12:00:14.04	6.791	-	50-200		-

Table A2 – *continued* Results of the F-WBSB data analysis (August 2017, August 2018 and September 2018) compared with the onboard GBM analysis. As an indication, other surveys that independently triggered on the same gamma-ray bursts as HXMT, Swift-BAT, Konus-Wind, Calet and MAXI are reported as well.

Search	Detectors Involved	Time (UT)	Trigger Duration (s)	SNR (av)	Energy band (keV)	GRB classification	Ref
			August 2017				
			bn170825784				
GBM onboard	n3,n5	18:49:11.04	2.048	5.1	47-291		Notice
F-WBSB	n3,n4	18:48:46.06	39.552	19.0	4-50		
F-WBSB	n4,n6,n7	18:48:48.11	38.656	15.8	4-900	long	Link
F-WBSB	n3,n4,n6	18:48:46.03	36.48	15.0	50-100		
F-WBSB	n3,n4,n6	18:49:03.74	18.944	15.6	50-900		
			bn170826369				
GBM onboard	n1,n2	08:51:07.51	0.016	7.5	47-291	short	Notice
F-WBSB			No data available				
Konus-WIND	-	08:51:08.41	0.114	-	50-200		Notice
			bn170826819				
GBM onboard	na,nb	19:38:56.48	1.024	4.5	47-291	long	Notice
HXMT	-	19:38:58.00	10.12	-	80-800		Notice
F-WBSB			No data available				
Konus-WIND	-	19:39:02.55	9.758	-	50-200		Notice
			bn170827818				
GBM onboard	n0,n2	19:38:04.46	0.512	4.8	47-291	short	Notice
F-WBSB	n0,n1	19:38:03.44	1.408	9.9-10.0	4-900		Link
F-WBSB	n0,n2,n5	19:38:04.10	0.768	6.1	50-900		
Konus-WIND	-	19:38:06.84	0.178	-	50-200		Notice
			bn170829414				
GBM onboard	n7,nb	09:56:30.58	0.512	4.8	47-291		Notice
F-WBSB	n6,n7,n9	09:56:30.15	47.616	13.2	4-50		
F-WBSB	n6,n7	09:58:04.99	3.968	7.0	4-50		
F-WBSB	n6,n7,n8,n9,nb	09:56:29.25	49.28	16.7	4-900	long	Link
F-WBSB	n6,n7	09:58:05.12	3.84	6.3	4-900		
F-WBSB	n6,n7,n8,n9	09:56:29.00	43.776	13.1	50-100		
F-WBSB	n6,n7,n8,n9,nb	09:56:29.25	43.648	15.4	50-900		
			bn170829674				
GBM onboard	n8,n9,nb	16:10:03.16	0.256	4.9	47-291		Notice
F-WBSB	n6,n7,n9	16:10:02.56	43.776	9.3	4-50		
F-WBSB	n6,n7,n8,n9,na,nb	16:10:02.82	45.696	11.9	4-900	long	Link
F-WBSB	n6,n7,n9,na,nb	16:10:02.82	10.624	11.9	50-100		
F-WBSB	n6,n7,n8,n9,na,nb	16:10:02.82	13.312	13.2	50-900		
Konus-WIND	-	16:10:07.68	44.744	-	50-200		-
			bn170830069				
GBM onboard	n7,nb	01:38:44.23	1.024	4.7	47-291		Notice
F-WBSB	n6,n9	01:39:03.62	1.664	6.8	4-50		
F-WBSB	n4,n6,n8,n9	01:38:59.65	14.848	11.7	4-900	long	Link
F-WBSB	n9,nb	01:39:00.06	13.440	10.7	50-100		
F-WBSB	n6,n7,n8,n9,na,nb	01:38:59.41	14.208	12.6	50-900		
			bn170830135				
GBM onboard	n9,na	03:14:01.95	0.512	4.7	47-291		Notice
F-WBSB	n9,na	03:14:01.15	12.416	10.9	4-50	long	
F-WBSB	n2,n9,na,nb	03:14:00.64	45.312	8.1	4-900		Link
F-WBSB	n9,na	03:14:01.03	6.272	15.0	50-900		
F-WBSB	n2,n9,na	03:14:01.16	6.144	9.0	50-100		
MAXI	-	03:15:29	-	-	4-10		Notice
Astrosat-CZT	-	03:14:00	-	-	4-200		Notice
			bn170830328				
GBM onboard	n3,n4	07:51:51.11	2.048	5.1	47-291		Notice
F-WBSB	n3,n4	07:51:47.78	9.216	14.2	4-50	long	
F-WBSB	n3,n4,n5,n8	07:51:48.80	8.832	15.7	4-900		Link
F-WBSB	n1,n5,n8	07:51:48.30	8.832	6.2	50-100		
F-WBSB	n5	07:51:48.94	7.808	10.9	50-900		
CALET	-	07:51:52.37	4.0	11.6	4-100		Notice
Konus-WIND	-	07:51:50.16	80.509	-	50-200		-

Table A2 – *continued* Results of the F-WBSB data analysis (August 2017, August 2018 and September 2018) compared with the onboard GBM analysis. As an indication, other surveys that independently triggered on the same gamma-ray bursts as HXMT, Swift-BAT, Konus-Wind, Calet and MAXI are reported as well.

Search	Detectors Involved	Time (UT)	Trigger Duration (s)	SNR (av)	Energy band (keV)	GRB classification	Ref
			August 2017				
			bn170831179				
GBM onboard	n0,n3	04:18:11.13	2.048	4.9	47-291		Notice
F-WBSB	n0,n3,n4,n5	04:18:09.22	58.88	49.7	4-50		
F-WBSB	n0,n1,n3	04:18:03.84	64.896	49.6	4-900	long	Link
F-WBSB	n0,n1,n3,n4,n5	04:18:14.08	51.328	26.4	50-100		
F-WBSB	n0,n1,n3	04:18:14.34	77.952	23.4	50-900		
Konus-WIND	-	04:18:32.76	48.859	-	50-200		-
			August 2018				
			bn180809485				
GBM onboard	n9,nb	11:38:12.08	1.024	6.0	47-291		Notice
F-WBSB	n6,na,nb	11:38:09.98	17.408	11.8	4-50		
F-WBSB	n6,n9	11:38:06.92	14.976	11.8	50-100	long	Link
F-WBSB	n6,n7,n9,na	11:38:08.97	24.704	13.4	50-900		
F-WBSB	n6,n9,nb	11:38:08.96	19.328	18.0	4-900		
MAXI	-	11:38:25	-	-	2-4		Notice
			bn180810278				
GBM onboard	n8,nb	06:40:46.74	2.048	5.1	47-291		Notice
F-WBSB	n7,n8,nb	06:40:44.35	8.064	10.3	4-50		
F-WBSB	n8,nb	06:40:45.00	14.848	9.2	50-100	long	Link
F-WBSB	nb	06:40:44.10	15.744	11.1	50-900		
F-WBSB	n7,n8,nb	06:40:44.35	15.36	13.4	4-900		
			bn180812349				
GBM onboard	n1,n2	08:22:30.31	0.128	5.1	47-291	long	Notice
F-WBSB	n0	08:22:29.70	21.76	7.3	4-900		Link
Swif-BAT	-	08:22:30.23	2.048	11.2	25-100		Notice
			bn180814505				
GBM onboard	n6,n9,nb	12:06:54.07	2.048	4.7	47-291		Notice
F-WBSB	n6	12:07:35.62	11.008	6.3	4-900	long	Link
F-WBSB	n9	12:06:51.00	3.328	6.4	4-900		
			bn180816088				
GBM onboard	n0,n1,n2	02:07:18.91	1.024	4.9	47-291		Notice
F-WBSB	n0,n1,n2,n5	02:07:16.93	42.496	60.3	4-50		
F-WBSB	n0,n1,n5	02:07:17.95	43.008	26.3	50-100	long	Link
F-WBSB	n0, n1, n3, n5	02:07:17.83	40.192	25.9	50-900		
F-WBSB	n0,n1,n2,n3,n5	02:07:16.93	41.472	63.7	4-900		
HXMT	-	02:07:18.91	36.58	-	80-800		-
Konus-WIND	-	02:07:34.83	31.261	-	50-200		-
			bn180816930				
GBM onboard	n3,n4	22:19:53.32	1.024	5.4	47-291		Notice
F-WBSB	n3,n4	22:19:51.23	9.984	11.1	4-50		
F-WBSB	n3,n4	22:19:51.37	9.6	9.0	50-100	long	Link
F-WBSB	n3,n4	22:19:51.49	9.728	9.6	50-900		
F-WBSB	n3,n4,n5	22:19:51.49	10.368	11.9	4-900		
			bn180818179				
GBM onboard	n2,n5	04:17:58.30	0.128	5.7	47-291	long	Notice
F-WBSB	n2	04:17:56.67	0.768	5.1	50-900		Link
			bn180818520				
GBM onboard	n2,n5	12:28:58.24	0.128	5.7	47-291		Notice
F-WBSB	n0,n1,n2	12:28:44.74	30.848	6.6	4-50	long	
F-WBSB	n1,n5	12:28:47.30	21.12	6.6	4-900		Link
F-WBSB	n2,n5	12:30:37.63	19.712	6.4	4-50		
F-WBSB	n2,n5	12:30:38.66	22.272	6.4	4-900		
Swif-BAT	-	12:30:18.55	128	10.2	15-50		Notice

Table A2 – *continued* Results of the F-WBSB data analysis (August 2017, August 2018 and September 2018) compared with the onboard GBM analysis. As an indication, other surveys that independently triggered on the same gamma-ray bursts as HXMT, Swift-BAT, Konus-Wind, Calet and MAXI are reported as well.

Search	Detectors Involved	Time (UT)	Trigger Duration (s)	SNR (av)	Energy band (keV)	GRB classification	Ref
			August 2017				
			bn180821653				
GBM onboard	n3,n6	15:40:39.22	4.096	4.7	47-291	long	Notice
F-WBSB	n3	15:41:32.04	0.768	36.3	4-900		Link
			bn180822423				
GBM onboard	n3,n4,n7	10:08:27.90	0.256	5.1	47-291		Notice
F-WBSB	n3,n4	10:08:26.82	8.704	16.8	4-50		
F-WBSB	n3,n4,n6,n7	10:08:26.44	8.448	12.1	50-100	long	Link
F-WBSB	n3,n4,n5,n6,n7	10:08:26.56	9.344	10.5	50-900		
F-WBSB	n3,n4,n6	10:08:26.56	8.448	17.6	4-900		
			bn180822562				
GBM onboard	n0,n1	13:28:34.50	0.256	5.1	47-291		Notice
F-WBSB	n0,n1	13:28:35.01	2.816	23.0	4-50		
F-WBSB	n0,n3	13:28:34.00	3.968	13.6	50-100	long	Link
F-WBSB	n0,n1,n3	13:28:33.48	4.48	16.5	50-900		
F-WBSB	n0,n1,n3	13:28:33.22	4.864	21.5	4-900		
HXMT	-	13:28:34.05	3.677	-	80-800		-
Konus-WIND	-	13:28:34.47	128.9	-	50-200		-
			bn180823442				
GBM onboard	n1,n9	10:36:39.23	1.024	5.5	47-291		Notice
F-WBSB	n6,n9	10:36:35.14	20.9	9.6	50-900	long	Link
F-WBSB	na,nb	10:36:36.42	7.7	8.4	4-900		
			bn180826055				
GBM onboard	n1,n9	01:19:15.54	2.048	4.5	47-291		Notice
F-WBSB	n1,n6	01:20:12.23	21.76	7.85	4-50		
F-WBSB	n0,n4,na	01:20:06.59	34.816	14.1	50-900	long	Link
F-WBSB	n1,n2,n6,nb	01:20:14.14	22.784	15.45	4-900		
Konus-WIND	-	01:20:29.84	211.78	-	50-200		-
			bn180828790 - NOT A GRB				
GBM onboard	n9,na,nb	18:57:39	0.519	4.9	47-291		Notice
F-WBSB			No data available				
Swif-BAT	-	18:57:22.49	1.024	120.68	50-350	-	Notice
HXMT	-	18:57:26.58	7.607	-	80-800		-
Konus-WIND	-	18:57:30.02	8.334	-	50-200		-
			September 2018				
			bn180905400				
GBM onboard	n9,nb	09:36:09.67	1.024	5.9	47-291		Notice
F-WBSB	n9,na	09:36:10.18	6.016	8.3	4-50		
F-WBSB	n9,na	09:36:08.77	6.016	10.8	4-900	long	Link
F-WBSB	n9,na	09:36:08.52	5.12	8.9	50-100		
F-WBSB	n1,n9,na	09:36:08.51	4.608	7.5	50-900		
			bn180906597				
GBM onboard	n1,n2	14:19:51.78	0.256	4.5	47-291		Notice
F-WBSB	n0,n1,n2,n5	14:19:52.26	14.72	12.1	4-50		
F-WBSB	n1,n2,n5	14:19:50.21	12.288	17.3	4-900	long	Link
F-WBSB	n5	14:19:50.35	9.216	12.7	50-100		
F-WBSB	n0,n1,n2,n5	14:19:49.83	9.216	12.6	50-900		
			bn180906759				
GBM onboard	n6,nb	18:12:25.94	0.512	5.1	47-291		Notice
F-WBSB	n6,n7,n8,n9,nb	18:12:25.02	11.136	13.8	4-50		
F-WBSB	n6,n7,n8,n9,nb	18:12:25.15	10.112	22.7	4-900	long	Link
F-WBSB	n6,n7,n8,n9,nb	18:12:25.29	7.168	15.3	50-100		
F-WBSB	n6,n8,n9,nb	18:12:25.17	6.4	19.3	50-900		
Konus-WIND	-	18:12:27.92	6.613	-	50-200		-

Table A2 – *continued* Results of the F-WBSB data analysis (August 2017, August 2018 and September 2018) compared with the onboard GBM analysis. As an indication, other surveys that independently triggered on the same gamma-ray bursts as HXMT, Swift-BAT, Konus-Wind, Calet and MAXI are reported as well.

Search	Detectors Involved	Time (UT)	Trigger Duration (s)	SNR (av)	Energy band (keV)	GRB classification	Ref
August 2017							
bn180906988							
GBM onboard	n5,n6	23:42:34.16	0.256	5.2	47-291		Notice
F-WBSB	n6,n7	23:42:33.66	3.712	12.5	4-50	long	Link
F-WBSB	n6,n7	23:42:33.66	3.84	13.5	4-900		